Nanoscale ordering of polymer adsorbed on nanotubes

Simcha Srebnik*, Inna Gurevitz, and Stanislav Levchenko, Technion – Israel Institute of Technology, Haifa, Israel 32000

Abstract

We study the interaction of a dilute solution of semiflexible polymers with a weakly attractive infinitely long cylinder (i.e., nanotube) using Monte Carlo simulation. Apart for bending stiffness of the polymer chains, the only interactions considered in our model are weakly attractive short-ranged Lennard-Jones interactions between the monomers and with the surface. These nonspecific interactions are found to result in stable helical and multi-helical adsorbed conformations for semiflexible chains. Adsorption of these chains is found to occur in a sequential manner through tight wrapping of the polymer around the nanotube. Adsorption occurs quickly and is characterized by a sharp peak in the heat capacity. A second transition follows whereby opening and reorganization of the adsorbed chains into nearly perfect helices and multiple helices. Extension of the model to block and triblock copolymers reveals rich conformational behavior. These results are discussed on physical grounds and implications towards polymer-carbon nanotube composites are offered.

Keywords: Monte Carlo, polymers, adhesion, carbon nanotubes, block copolymers

* Email: simchas@technion.ac.il. Current address: Fischell Department of Bioengineering, University of Maryland, College Park, MD 20742

It is well known that carbon nanotubes (CNTs) possess extraordinary properties, such as regular electronic structure and high mechanical strength. However, since in their pristine state CNTs exist in a disordered agglomerated mass due to van der Waals (vdW) interactions (on the order of 0.5-1 eV per nm of nanotube-nanotube contact [1, 2]), the theoretical potential of their extraordinary properties falls far short of the actual performance [3]. The first challenge is, therefore, to obtain a homogeneous dispersion of CNTs for practical applications.

Regular helical wrapping of nanotubes, displayed by a number of polymers [4-8], may be used advantageously in the dispersion and control of properties of CNT/polymer composites, for example, through the helical pitch which directly controls the linear charge density of the complex and is predicted to be an important parameter controlling separation in ion-exchange chromatography [9, 10]. Recently, using coarse-grained MC simulations, in which only short-ranged weakly attractive nonbonded interactions were considered, we have shown that semiflexible chains will adsorb in nearly perfect helices on CNTs [11-13]. When multiple chains are allowed to adsorb on CNTs, simulations predict the formation of multiple helices [12, 13].

Block copolymers offer an additional parameter over homopolymers that can be used to control the distance between NTs, and thus may be used to tailor the structure and performance of polymer/NT composites.[14] In a recent study,[13] we showed that a sufficiently long hydrophobic block (H) will adsorb in a helical manner, while the polar block (P) extends to the bulk. Triblock (HPH) copolymers may provide additional advantage, in principle, by allowing for the formation of loops, anchored to the CNT surface by the wrapped hydrophobic blocks. The polar loops extending to the bulk can in principle entangle with free polymer, leading to strong adhesion between the CNTs and bulk polymer.

In this work, we utilize a minimalist Monte Carlo model in order to concentrate on the physical effects that drive long polymer chains to associate with CNTs and adopt ordered adsorbed conformations. The monomers are modeled as soft spheres, with Lennard-Jones (LJ) interaction potential between non-bonded monomers,

$$\frac{U_{LJ}}{kT} = 4\varepsilon_{ij}\left[\left(\frac{\sigma_{ij}}{r_{ij}}\right)^{12} - \left(\frac{\sigma_{ij}}{r_{ij}}\right)^{6}\right] \qquad (1)$$

where k is the Boltzmann constant, T is the temperature, ε_{ij} is the average 2-body LJ interaction parameter between monomers i and j ($\varepsilon_{ij} = \left(\varepsilon_{ii}\varepsilon_{jj}\right)^{1/2}$), σ_{ij} is the average effective size of monomers i and j ($\sigma_{ij} = \left(\sigma_i + \sigma_j\right)/2$), and r_{ij} is the distance between the two interacting nonbonded monomers. The well potentials used for the hydrophobic and polar interactions are $\varepsilon_H = 1$ and $\varepsilon_P = 0.01$, respectively. A cut-off radius of $2^{1/6}\sigma$ for the monomer-monomer interactions is used to allow for the effect of short-range attractive forces at a low computational cost. We note that for the monomer-monomer LJ interactions, the potential cut-off has a minor affect on chain conformational behavior when compared with the bending potential (Eq. 2, below) at the temperature, chain length, and concentration studied, especially for the stiffer chains. Thus, the

attractive well of the potential really only comes into play when the chains are adsorbed on the cylinder.

Chain stiffness is modeled by the following harmonic expression for the energy required to bend the angle θ formed between consecutive bond vectors,

$$U_b/kT = \kappa(\cos\theta - 1)^2 \qquad (2)$$

where κ characterizes the resistance of the bond angle θ_j about monomer j to bending. is defined by $\cos\theta_j = \mathbf{b}_{j-1} \cdot \mathbf{b}_j \Big/ \left(\left\|\mathbf{b}_{j-1}\right\|\mathbf{b}_j\right)$, where $\mathbf{b}_j = r_{j+1} - r_j$, and r_j is the absolute position of monomer j. The bending stiffness parameter κ appearing in Eq. 2 can be easily related to the persistence length, l_p, through a bond-angle correlation function which decays exponentially with l_p, thereby obtaining a power law dependence of l_p on κ [15-18]. Note that using $\cos\theta$ instead of θ in Eq. 2 simply provides a different correlation between κ and the persistence length of the polymer, but simplifies the computational calculation by avoiding the use of the inverse cosine function. These simulation parameters correspond to good solvent conditions.

Since CNTs exhibit an even charge distribution [19], electrostatic interaction between nanotubes and polymers is relatively weak, and therefore in the absence of chemical functionalization, the polymer-CNT interaction is governed by van der Waals forces [20, 21]. Therefore, we model the CNT as a smooth infinitely long and impenetrable cylindrical shell with a continuous LJ potential field averaged over the tube length. The polymer-tube interactions are obtained by integrating the dimensionless LJ potential over the length of the tube [17, 22], to obtain a potential that depends on tube dimensions (inner radius ρ_i and outer radius ρ_o) and the perpendicular distance of a monomer from the surface of the tube, D. Integration of Eq. 1 over the vertical z-axis of the tube yields and an analytical equation, whose integration over the radial and azymuthal axes needs to be carried out numberically. The resulting potential was adjusted such that the potential minimum of tubes of different radii correspond to the potential minimum of a tube with ρ_o=2σ in order to concentrate on the effect of surface curvature.

Simulations were carried out on chains consisting of N_m monomer units consisting of b blocks, where each block is made up of N_H hydrophobic (H) segments or N_P polar (P) segments. Bond length was taken to be 1σ in all our simulations. All segments were taken to be of equal size, σ. A cubic simulation box with periodic boundary conditions was considered with the nanotube placed in the center of the box, aligned along the z-axis. The simulation is initialized by placing N_c identical chains randomly within the box. We use N_c=3 for the homopolymer and N_c=1 for the block copolymer (unless otherwise stated). Equilibration is achieved using a combination of reptation and kink-jump moves [23], tried with approximately 0.1 and 0.9 probability, respectively, during the production stage of the simulation. The move probability is adjusted at the course of equilibration to achieve approximately 50% Metropolis acceptance rate. To ensure equilibration, 10^6 MC steps are performed prior to calculating average properties. Averages are calculated over an additional 10^6 - 10^7 MC steps, sampled every 10^2 MC steps. Although we studied nanotubes of various radii, we concentrated on ρ = 2σ, which corresponds to the dimension of single-walled CNTs [12].

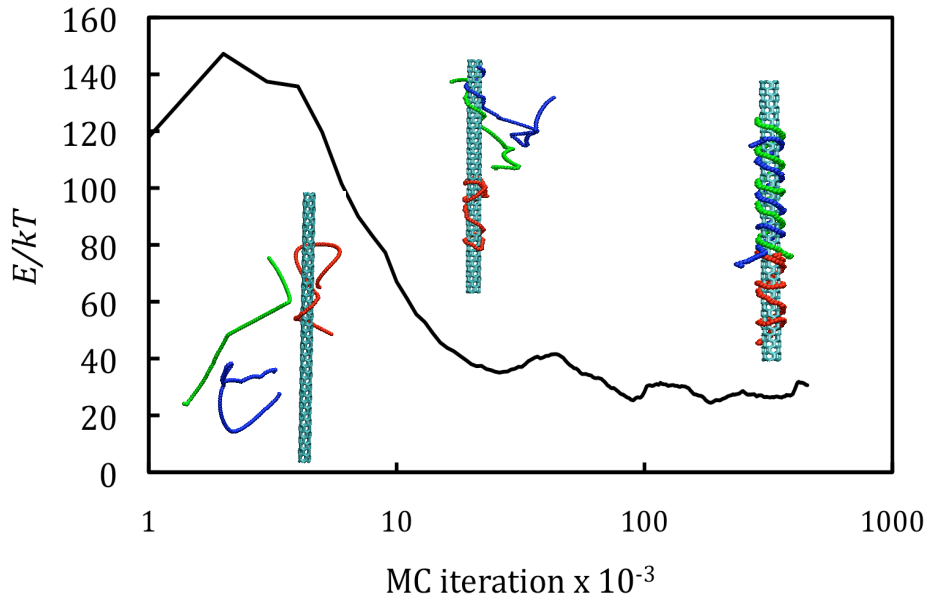

Figure 1. Energy as a function of simulation time; $\kappa = 40$, $\rho = 2\sigma$, $N_m = 100$, $kT = 1$. Snapshots, from left to right, correspond to typical conformations at these conditions after 10^3 iterations, 10^4 iterations, and 10^5 iterations, respectively.

Recently, we have shown that there exists a range of parameters for which polymers will adsorb on CNTs in an ordered helical manner [11, 13, 17]. As seen in **Figure 1**, the energy reaches its equilibrium value quite quickly, whereby nearly perfect helical conformations are observed. Adsorption is reversible with temperature (**Figure 2**), indicating that the observed helical conformations are a thermodynamically stable state, also at finite temperatures. Desorption of the polymers with increasing temperature has also been reported experimentally [5].

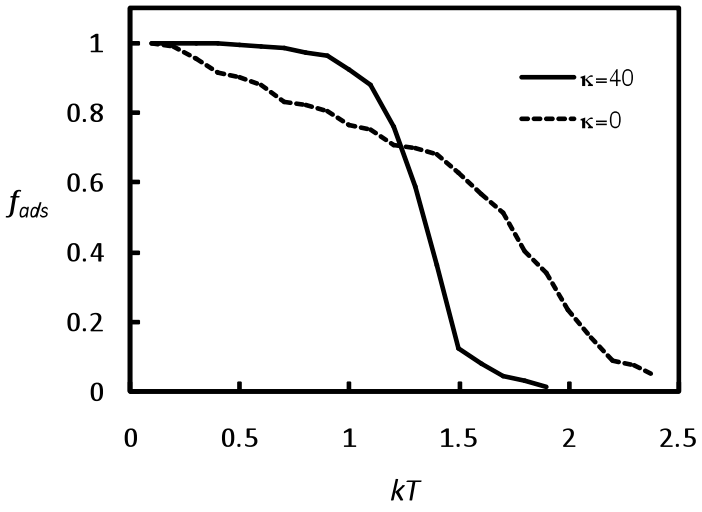

Figure 2. Adsorbed fraction as a function of temperature; $\rho = 2\sigma$, $N_m = 100$.

During the course of the simulation, the polymers spiral up and down the surface of the tube. This behavior suggests that the polymers adopt a conformation with an optimal pitch. The helical pitch is predicted to be an important parameter controlling, e.g., separation in ion-exchange chromatography since it directly controls the linear charge density of the polymer-CNT surface, and thus strongly influences the electrostatic field near the surface [19, 24]. Thus, nonspecific association that is responsible fore helical wrapping may also result in an optimal pitch for a particular polymer-CNT configuration. That an optimal helical pitch may be determined by nonspecific structure and interactions is important since all known preparations of CNTs give mixtures of nanotube chiralities [25].

The dependence of the adsorbed fraction and of α on chain length obtained from the simulation is shown in **Figure 3**. The dashed line represents the adsorption transition marking the approximate location of the peak in the fluctuations C_a of the adsorbed fraction, i.e., $C_a = \langle f_{ads}^2 \rangle - \langle f_{ads} \rangle^2$. **Figure 3**a suggests that short chains remain largely in the bulk, while longer chains adsorb readily. Chain length then plays an important factor in determining the adhesion between the polymers and CNT, with the transition between oligomeric behavior to polymer behavior in this study occurring at $N_m \approx 15$ (dashed line). Polymer chains are therefore expected to be much more efficient at solubilizing CNTs then their oligomeric counterparts [6]. We also learn from **Figure 3**b that oligomeric chains of all flexibilities as well as long flexible polymers adsorb in random orientations ($\alpha = \pi/2$), while the longer stiff polymers adsorb in a conformation characterized by $\alpha < \pi/2$. The random adsorbed orientation of the short stiff oligomers results from their relatively low entropic state (compared with a long polymer chain), allowing oligomers to readily fluctuate between and adsorbed and desorbed states.

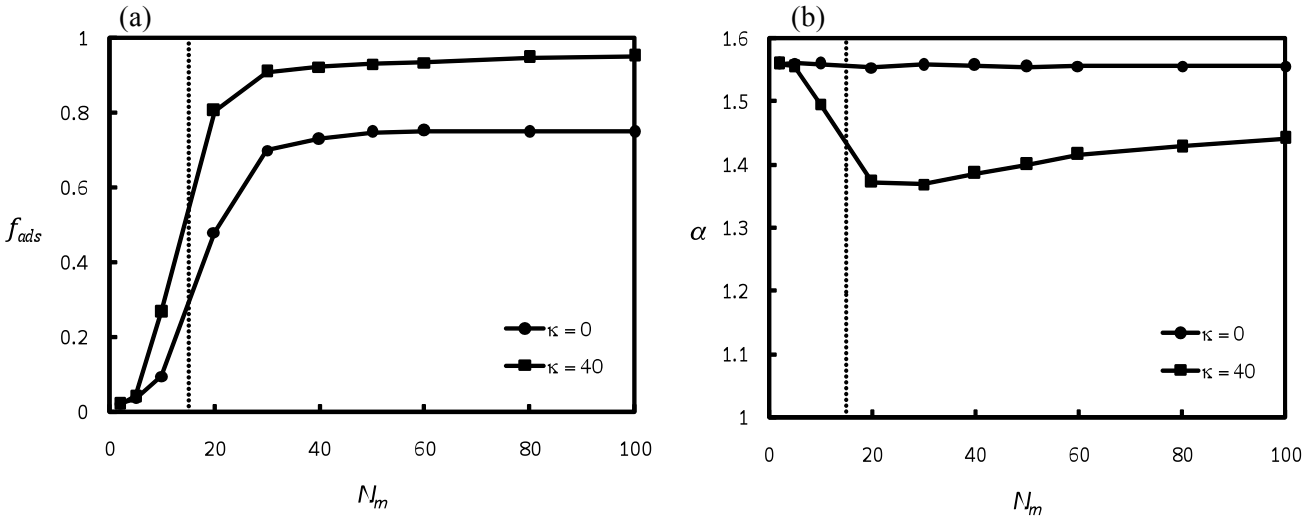

Figure 3. (a) Adsorbed fraction and (b) helical pitch as function of chain length; $\rho = 2\sigma$, kT=1. The dotted lines represents the adsorption transition obtained from the peak in the fluctuations of the adsorbed fraction.

The average pitch angle α of the adsorbed polymers is found to be nearly independent of chain length for sufficiently long chains (**Figure 3**). α can be approximated from the Kratky-Porod [26] (KP) wormlike chain assumption that the angle θ formed by bond vectors separated by x segments decays exponentially, $\langle \cos\theta_x \rangle \sim \exp\left(-xl/l_p\right)$, where l_p is the persistence length of the chain. Assuming that the optimal conformation occurs when the average bond angle between two consecutive segments (x = 1) corresponds to the average bond angle θ of the adsorbed polymer. The relation between the pitch angle α and bond angle θ can then be obtained from geometric considerations, and may be shown to be independent of chain length [27]. The prediction of the helical pitch thus obtained as a function of chain stiffness is shown by the dashed curve of **Figure 4**. The symbols show the calculated pitch angle from simulations, using the relation $l_p \approx \kappa^{0.6}$ [12]. A better agreement is obtained when θ is corrected by 2° (solid curve). That is, the adsorbed chains have a somewhat smaller bending angle (they are more flexible) then predicted by the unconfined KP model. The probable cause is the interaction with the CNT surface, which competes with the bending interactions and thereby reduces the effective size of the chain. The transition to extended conformations ($\alpha < \pi/2$) in **Figure 4** occurs when chain stiffness, determined from the average bending angle, $\theta = \cos^{-1}\left(-e^{-l/l_p}\right)$, approximately equals the minimum radius of curvature of the cylinder, $\theta_c = 2\cos^{-1}\left(l/2\rho\right)$. Polymers with l_p beyond this critical value will adsorb in extended helical conformation to reduce the effect of surface curvature.

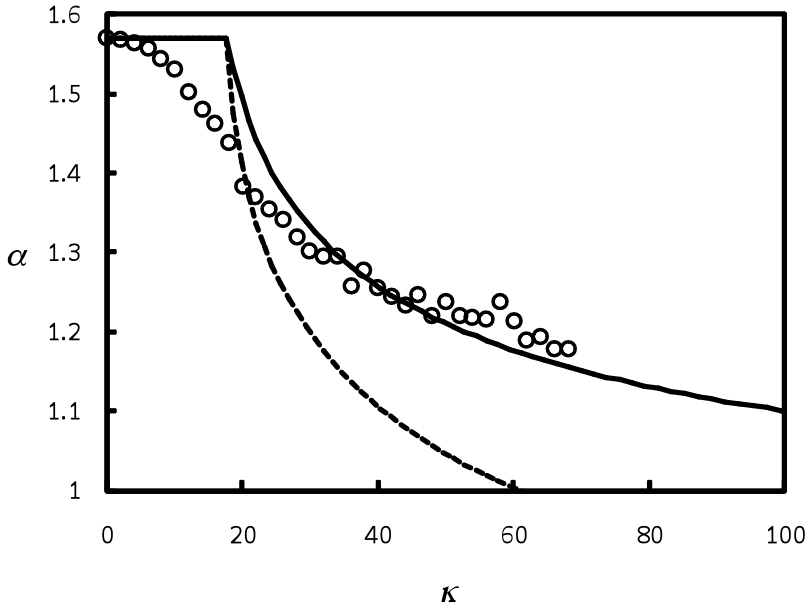

Figure 4. Helical pitch as a function of κ. Symbols show simulation results ($\rho = 2\sigma$, kT=1), dashed curve shows model predictions for the same conditions, and solid curve shows model predictions with a 2° correction to α.

Our previous simulations indicate that semiflexible homopolymers under the conditions studied adsorb in a monolayer on the surface of the CNT, for the range of concentrations studied [13]. Such conformation may not be ideal for polymer reinforcement, where strong adhesion between the polymer matrix and CNT is required. For such applications, block copolymers (BCPs) consisting of monomers with different solvent selectivity may provide a stronger interface between the CNT and polymer [28]. In such a scenario, one block is anchored to the CNT surface through strong physical association, while the other block extends to solution. This configuration not only provides steric repulsion between CNTs but also increases adhesion between the CNT-polymer interface [14] by allowing for entanglement between the adsorbed polymers and matrix polymers.

We studied the adsorption and wrapping mechanism of diblock and triblock copolymers on CNTs consisting of hydrophobic (H) blocks that favorably interact with the CNT ($\varepsilon_H = 1$) and 'polar' (P) blocks that interact with the CNT through weakly attractive interactions ($\varepsilon_P = 0.01$). Such a choice of interactions represents adsorption in a hydrophobic solvent, and results in strong microphase separation of the hydrophobic and polar segments of the polymer in absence of the CNT [29]. In general, adsorbed BCPs show significant loss of order when compared to homopolymers under the same conditions, though helical conformations of the H blocks may also be observed (Figure 5). However, at the relatively short simulation times considered, helical conformations appear to occur fortuitously if H segments near the interface between the two blocks adsorb first, allowing for sequential wrapping of the other H segments. Thus, a mixture of helical and ordered configurations might be expected, as has also been reported experimentally for alternating copolymers [30]. Similar to the homopolymer, the randomly adsorbed state of the copolymer is likely to be a metastable state. However, for the copolymer, rearrangement to the helical state requires significantly longer (simulation) times due to the competing interactions of the polar block. Nonetheless, the possibility of formation of loops with the triblock copolymers, shown in Figure 5, might offer particular advantage towards interface reinforcement, by addressing both adhesive and cohesive failure in polymer/CNT composites.

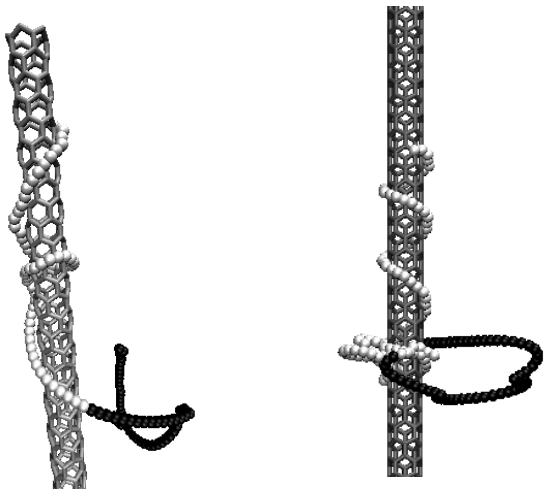

Figure 5. Simulation snapshots of diblock (left) and triblock (right) copolymer-CNT systems; $\kappa_H = \kappa_P = 40$, $\rho = 2\sigma$, $N_m = 60$ per block.

References

1. Dyke, C.A. and J.M. Tour, Journal of Physical Chemistry A, 2004. **108**(51): p. 11151-11159.
2. Nap, R. and I. Szleifer, Langmuir, 2005. **21**(26): p. 12072-12075.
3. Bokobza, L., Polymer, 2007. **48**(17): p. 4907-4920.
4. Kim, O.K., et al., Journal of the American Chemical Society, 2003. **125**(15): p. 4426-4427.
5. Tang, B.Z. and H.Y. Xu, Macromolecules, 1999. **32**(8): p. 2569-2576.
6. Yuan, W.Z., et al., Macromolecules, 2008. **41**(3): p. 701-707.
7. Fu, C., et al., Macromolecular Rapid Communications, 2007. **28**(22): p. 2180-2184.
8. Dieckmann, G.R., et al., Journal of the American Chemical Society, 2003. **125**(7): p. 1770-1777.
9. Lustig, S.R., et al., Journal of Physical Chemistry B, 2005. **109**(7): p. 2559-2566.
10. Manohar, S., T. Tang, and A. Jagota, Journal of Physical Chemistry C, 2007. **111**(48): p. 17835-17845.
11. Kusner, I. and S. Srebnik, Chemical Physics Letters, 2006. **430**: p. 84-88.
12. Gurevitch, I. and S. Srebnik, Chemical Physics Letters, 2007. **444**(1-3): p. 96-100.
13. Gurevitch, I. and S. Srebnik, The Journal of Chemical Physics, 2008. **128**(14): p. 144901.
14. Shvartzman-Cohen, R., et al., Langmuir, 2004. **20**(15): p. 6085-6088.
15. Cerda, J.J., T. Sintes, and A. Chakrabarti, Macromolecules, 2005. **38**(4): p. 1469-1477.
16. Micka, U. and K. Kremer, Journal of Physics - Condensed Matter, 1996. **8**(47): p. 9463-9470.
17. Gurevitch, I. and S. Srebnik, Chemical Physics Letters, 2007. **444**: p. 96-100.
18. Kusner, I. and S. Srebnik, Macromolecules, 2007. **40**(17): p. 6432-6438.
19. Wall, A. and M.S. Ferreira, Physical Review B, 2006. **74**(23).
20. Yang, M.J., V. Koutsos, and M. Zaiser, Journal of Physical Chemistry B, 2005. **109**(20): p. 10009-10014.
21. Xie, Y.H. and A.K. Soh, Materials Letters, 2005. **59**(8-9): p. 971-975.
22. Milchev, A. and K. Binder, Journal of Chemical Physics, 2002. **117**(14): p. 6852-6862.
23. Baschnagel, J., J.P. Wittmer, and H. Meyer, *Monte Carlo Simulation of Polymers: Coarse-Grained Models*, in *Computational Soft Matter: From Synthetic Polymers to Proteins*, N. Attig, et al., Editors. 2004, John von Neumann Institute for Computing: Julich. p. 83-140.
24. Wall, A. and M.S. Ferreira, Journal of Physics-Condensed Matter, 2007. **19**(40).
25. Moniruzzaman, M. and K.I. Winey, Macromolecules, 2006. **39**(16): p. 5194-5205.
26. Kratky, O. and G. Porod, Recl. Trav. Chim. Pays-Bas, 1949. **68**: p. 1106.
27. Srebnik, S., Journal of Polymer Science Part B-Polymer Physics, submitted.
28. Vaisman, L., H.D. Wagner, and G. Marom, Advances in Colloid and Interface Science, 2006. **128**: p. 37-46.
29. Marrink, S.J., A.H. de Vries, and A.E. Mark, Journal of Physical Chemistry B, 2004. **108**(2): p. 750-760.
30. McCarthy, B., et al., Synthetic Metals, 2001. **121**(1-3): p. 1225-1226.
31. Strano, M.S., et al., Journal of Nanoscience and Nanotechnology, 2003. **3**(1-2): p. 81-86.